CHEMICAL ENGINEERING TRANSACTIONS
VOL. 117, 2025
A publication of AIDIC
The Italian Association of Chemical Engineering
Online at www.cetjournal.it
Guest Editors: Fabrizio Bezzo, Flavio Manenti, Gabriele Pannocchia, Almerinda di Benedetto

ISBN 979-12-81206-17-5; **ISSN** 2283-9216
DOI: 10.3303/CET25117167

Process Integration Approach for the Efficient Synthesis of Metal Boride Ceramics

Mariano Casu, Antonio M. Locci, Gabriele Traversari, Giacomo Cao, Roberto Orrù

Department of Mechanical, Chemical and Materials Engineering, University of Cagliari, Piazza d'Armi, 09123 Cagliari, Italy
roberto.orru@unica.it

Inspired by the principle of process integration, a novel Self-propagating High-temperature Synthesis (SHS) route based on the combination of direct (DR) and borothermal (BR) reactions is proposed in this work for the synthesis of transition metal diborides. The aim is to identify the proper operating conditions that maximize the use of cheaper metal oxides as starting reactants instead of elemental powders, while still guaranteeing the self-propagating character of the synthesis process, by taking advantage of the excess heat generated by the DR reaction. A theoretical analysis based on accurate thermodynamic description of the reacting system is performed to evaluate the adiabatic temperatures of the combined DR-BR process, under different pressure conditions, for the synthesis of TiB_2, ZrB_2, and HfB_2 transition metal diborides. The analysis outcomes have been validated by an experimental campaign, where SHS process was followed by a purification step to eliminate undesired byproducts (B_2O_3).

1. Introduction

Given their peculiar properties, transition metal diborides (TMBs) like MeB_2 (Me=Ti, Zr, Hf, etc.) have attracted a significant interest for various advanced high-temperature applications, such as in aerospace (Fahrenholtz et al., 2016) or renewable energy sectors (Sani et al., 2017). These materials, which belong to the Ultra-High Temperature Ceramics (UHTCs), are usually synthesized by different solid-state pathways (Fahrenholtz et al., 2016). The direct reaction (DR) (Licheri et al., 2016) and the borothermal reaction (BR) (Guo et al., 2014) can be cited among the most used ones. The first route consists of the following reaction:

$$\mathrm{Me} + 2\mathrm{B} \rightarrow \mathrm{MeB_2} \quad (1)$$

while BR starts from the corresponding oxides using boron as reducing agent:

$$\mathrm{MeO_2} + \frac{10}{3}\mathrm{B} \rightarrow \mathrm{MeB_2} + \frac{2}{3}\mathrm{B_2O_3} \quad (2)$$

Eq(1) is strongly exothermic, while Eq(2) is generally endothermic or, for few diboride systems, slightly exothermic. Given the high enthalpy of formation of TMBs from their elements (Barin, 1995), Eq(1) can self-sustain along the reactants mixture after being locally ignited, with no additional energy requirement. This feature is the basis of the so called Self-Propagating High-Temperature Synthesis (SHS) process which has been extensively employed to synthesize various individual and multicomponent TMBs (Barbarossa et al., 2024). The advantage of BR reaction is the relatively low cost of transition metal oxides compared to elemental precursors, whereas its drawback is the high energy consumption of the synthesis process, which is performed in furnaces for several hours and at high temperatures (typically >1300 K) (Fahrenholtz et al., 2016). The advantage of the DR reaction performed via SHS is the lack of need of external energy supply and the rapidity of the process (~seconds). In contrast, the use of expensive elemental reactants makes it less convenient. The combination of these two synthesis pathways lays in the framework of process integration between exothermic and endothermic processes, which was successfully applied in other case studies (Kolios et al., 2002). The aim is then to maximise the use of metal oxides as starting reactants, while keeping the short processing times and energy saving advantages of the SHS technique. In this regard, the thermodynamic requirement to be generally satisfied by a reacting system to be self-sustaining is to possess an adiabatic temperature (T_a) equal or exceeding ~1800 K (Munir and Anselmi-Tamburini, 1989). In the present study, a thermodynamic analysis was developed to assess the T_a values when varying the relative contribution of BR and DR reactions to synthesize

Paper Received: 8 December 2024; Revised: 9 March 2025; Accepted: 22 April 2025
Please cite this article as: Casu M., Locci A., Traversari G., Cao G., Orrù R., 2025, Process Integration Approach for the Efficient Synthesis of Metal Boride Ceramics, Chemical Engineering Transactions, 117, 997-1002 DOI:10.3303/CET25117167

TiB_2, ZrB_2 and HfB_2 compounds. An experimental SHS campaign was also conducted to validate the reliability of the theoretical analysis, and to test the resulting optimal conditions.

2. Thermodynamic analysis

Defining Z as the molar fraction of the desired product obtained according to Eq(1) and $(1-Z)$ as the molar fraction obtained by Eq(2), the enthalpy balance for the adiabatic SHS process is:

$$0 = \Delta h_r + \upsilon_{MeB_2} q_{MeB_2} + (1-Z)\upsilon_{B_2O_3} q_{B_2O_3} \tag{3}$$

where the heat generated by the combined reactions can be described as:

$$\Delta h_r = \upsilon_{MeB_2} \Delta h_{f,MeB_2} + (1-Z)\upsilon_{B_2O_3} \Delta h_{f,B_2O_3} - (1-Z)\upsilon_{MeO_2} \Delta h_{f,MeO_2} \tag{4}$$

The expression of the adsorbed heat by the two products q_{MeB_2} and $q_{B_2O_3}$ variates according to the physical state of the latter ones. Specifically, it depends upon the value of the adiabatic temperature compared to the phase transition temperatures of the product:

$$q_{MeB_2} = \begin{cases} \int_{T_0}^{T_a} C_{P,MeB_2,s}\, dT & T_a < T_{m,MeB_2} \\ \int_{T_0}^{T_a} C_{P,MeB_2,s}\, dT + \Delta h_{s\to l,MeB_2} & T_a = T_{m,MeB_2} \end{cases} \tag{5}$$

$$q_{B_2O_3} = \begin{cases} \int_{T_0}^{T_a} C_{P,B_2O_3,s}\, dT & T_a < T_{m,B_2O_3} \\ \int_{T_0}^{T_a} C_{P,B_2O_3,s}\, dT + \Delta h_{s\to l,B_2O_3} & T_a = T_{m,B_2O_3} \\ \int_{T_0}^{T_{m,B_2O_3}} C_{P,B_2O_3,s}\, dT + \Delta h_{s\to l,B_2O_3} + \int_{T_{m,B_2O_3}}^{T_a} C_{P,B_2O_3,l}\, dT & T_{m,B_2O_3} < T_a < T_{b,B_2O_3} \\ \int_{T_0}^{T_{m,B_2O_3}} C_{P,B_2O_3,s}\, dT + \Delta h_{s\to l,B_2O_3} + \int_{T_{m,B_2O_3}}^{T_a} C_{P,B_2O_3,l}\, dT + \Delta h_{l\to g,B_2O_3} & T_a = T_{b,B_2O_3} \\ \int_{T_0}^{T_{m,B_2O_3}} C_{P,B_2O_3,s}\, dT + \Delta h_{s\to l,B_2O_3} + \int_{T_{m,B_2O_3}}^{T_{b,B_2O_3}} C_{P,B_2O_3,l}\, dT + \Delta h_{l\to g,B_2O_3} + \int_{T_{b,B_2O_3}}^{T_a} C_{P,B_2O_3,g}\, dT & T_a > T_{b,B_2O_3} \end{cases} \tag{6}$$

where:

$$C_{P,i,j}(T) = A_{i,j} + B_{i,j}T + C_{i,j}T^2 + D_{i,j}T^3 + E_{i,j}T^{-2};\ i = MeB_2, B_2O_3;\ j = s,l,g \tag{7}$$

Terms related to the gas or liquid state have been not considered for MeB_2, given the fact that the melting point of all three diboride systems corresponds to the maximum adiabatic temperature achievable in the limit case of Z=1. The Δh_r and molar latent heats were taken from literature (Barin, 1995). HfB_2 heat of fusion was not available, so it was assumed to be of the same order of magnitude as the ones of the two other diborides. i.e. $1 \cdot 10^5$ J/mol. C_P coefficients (Table 1) were regressed from heat capacity data reported in (Barin, 1995).

Table 1: Fitted parameters for the thermodynamic analysis (n.d.: not determined)

	B_2O_3	TiB_2	ZrB_2	HfB_2
$A_{i,s}$	3.67877	56.38012	64.21351	65.14057
$B_{i,s}$	0.28055	0.02586	0.00942	0.01842
$C_{i,s}$	$-2.65712\cdot10^{-4}$	$-3.3469\cdot10^{-6}$	$1.36824\cdot10^{-9}$	$-9.23555\cdot10^{-9}$
$D_{i,s}$	$1.05139\cdot10^{-7}$	$-4.80596\cdot10^{-14}$	$-2.18756\cdot10^{-13}$	$2.4396\cdot10^{-12}$
$E_{i,s}$	$-3.46430\cdot10^{5}$	$-1.74644\cdot10^{6}$	$-1.65824\cdot10^{6}$	$-1.88264\cdot10^{6}$
$A_{i,l}$	129.704	n.d.	n.d.	n.d.
$B_{i,l}, C_{i,l}, D_{i,l}, E_{i,l}$	0	n.d.	n.d.	n.d.
$A_{i,g}$	72.20376	n.d.	n.d.	n.d.
$B_{i,g}$	0.03472	n.d.	n.d.	n.d.
$C_{i,g}$	$-1.18376\cdot10^{-5}$	n.d.	n.d.	n.d.
$D_{i,g}$	$1.34692\cdot10^{-9}$	n.d.	n.d.	n.d.
$E_{i,g}$	$-1.34685\cdot10^{6}$	n.d.	n.d.	n.d.
α	17.40323	n.d.	n.d.	n.d.
β	$3.80644\cdot10^{4}$	n.d.	n.d.	n.d.
γ	-146.60608	n.d.	n.d.	n.d.

Regarding the phase transition temperatures, it is well known that the effect of pressure on melting temperatures is generally considered negligible. On the contrary, pressure can affect the boiling temperature of B_2O_3. Accordingly, the corresponding boiling temperature can be obtained by solving the following liquid-vapor equilibrium condition:

$$g_{B_2O_3,g}(T_{b,B_2O_3}, P) = g_{B_2O_3,l}(T_{b,B_2O_3}) \quad (8)$$

where the liquid phase has been assumed incompressible. The results obtained by solving Eq(8) were correlated through the following Antoine-like relation:

$$T_{b,B_2O_3} = \frac{\beta}{\alpha - \ln P} - \gamma \quad (9)$$

and the fitted parameters are also reported in Table 1. The non-linear algebraic equations (3)-(9) were solved by MATLAB® software.

3. Materials and methods

To properly validate the proposed model, SHS experiments were performed starting from Hf (Alfa Aesar, < 44 μm, 99.6% purity), Zr (Alfa Aesar, APS 2–3 μm), Ti (Thermo Scientific, < 44 μm, 99% purity), HfO_2 (Alfa Aesar, < 44 μm, 99% metal basis excluding Zr, Zr≤1.5%), ZrO_2 (Alfa Aesar, < 44 μm, 99% metal basis excluding Hf, HfO_2=2%), TiO_2 (Sigma Aldrich, 99% purity) and B (amorphous, Sigma Aldrich, 95% purity) reactants. Powders were either mixed for 20 min (ball-to-powder weight ratio, BPR=0.2), using plastic vials, and agata balls with a BML-2 roller bank (Witeg, Germany) or ball milled for 1h (BPR=1) by means of a SPEX 8000 (SPEX CertiPrep, USA) device with stainless steel vials and balls. SHS runs were conducted under 2 bar Argon atmosphere, and the resulting products were pulverized with 1h ball milling (BM) treatment using the SPEX 8000 equipment (BPR=2). Further details can be found elsewhere (Barbarossa et al., 2024).

The composition of SHS products was determined by X-Ray Powder Diffraction (XRD) analysis using a D8 (Brucker, Germany) diffractometer (Bragg-Brentano geometry) equipped with a rotating copper anode (Cu Kα radiation λ=1.5418 nm) working at 40kV and 100mA. The analysis was performed in the 20°-80° 2θ range, with a step-size of 0.015° and 0.2 seconds for each step.

The high temperatures encountered during SHS should lead to the evaporation of B_2O_3 but its presence in the synthesis product cannot be excluded. It should be noted that boria, B_2O_3 (solubility in water=2.2 g/100g, Green and Perry, 2007) usually reacts with air humidity to form crystalline boric acid, H_3BO_3 (solubility in water=5.04 g/100g, Green and Perry, 2007). Thus, to assess the presence of residual byproducts, the reacted powders were analyzed via XRD after being in contact with air for 1 and 28 days after synthesis. As literature suggests (Wu et al. 2019), given the high solubilities of boria and boric acid in H_2O, their removal was performed by treating the powders with distilled water at room temperature, followed by a filtering step.

4. Results and Discussion

Figure 1 shows the effect of Z on the adiabatic temperature of the reacting systems investigated in this work. It can be clearly seen that T_a increases as the fraction of the direct exothermic reaction augments. It is worth mentioning that the predicted adiabatic temperatures for the case of Z =1 (or Z =100%)
agree with the literature data (Munir and Anselmi-Tamburini, 1989).

The influence of B_2O_3 evaporation on T_a is reported in Figure 1. Horizontal segments indicate Z ranges where $T_a = T_{b,B_2O_3}$. It can be seen that, as P increases, the effect of B_2O_3 boiling on T_a shifts to higher temperature and Z values. The minimum values of Z (Z_{min}) that fulfill the adiabatic temperature constrain of $T_a \geq 1800$ K are indicated by the circles in Figure 1 and correspond to 6.78% for TiB_2 (Figure 1a), 43.73% for ZrB_2 (Figure 1b), and 50.26% for HfB_2 (Figure 1c). For each Z_{min} value, the minimum pressure (P_{min}) required to retain B_2O_3 in the liquid state during the process can be also calculated according to Eq(9). The resulting P_{min} corresponds to the vapor pressure of B_2O_3 at 1800 K (0.0036 bar). The condition P > 0.0036 bar makes the heat generated by the direct reaction completely available to sustain the borothermal reaction, instead of being partially consumed by B_2O_3 boiling. Thus, the thermodynamic analysis provides the minimum Z value requested to guarantee the SHS regime as well as the minimum pressure level needed to maintain B_2O_3 in the liquid state.

The theoretical predictions were experimentally tested under P = 2 bar. This value allows to minimize oxygen contamination inside the chamber while limiting technical complexity. A dedicated study was performed to verify the self-sustaining character of the process. The results obtained for the case of TiB_2 are reported in Figure 2, where the measured reaction front propagation velocities are also shown as a function of Z.

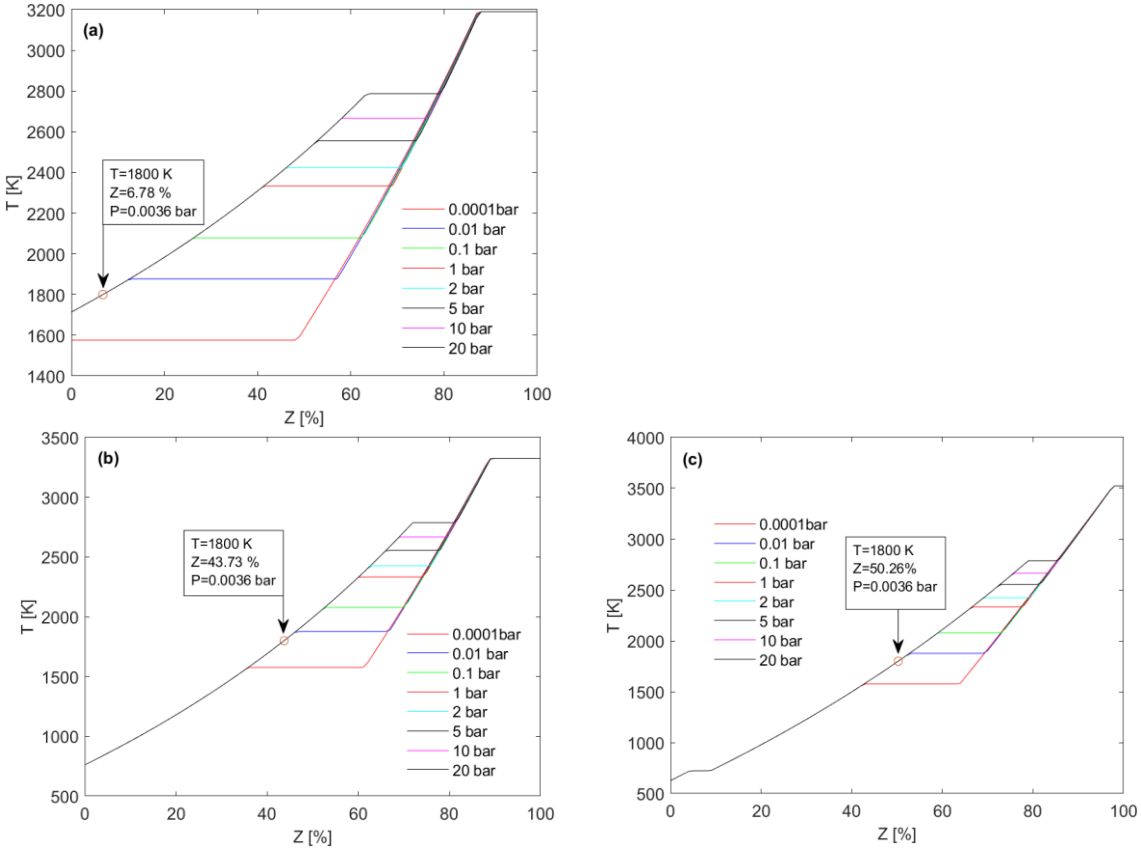

Figure 1: Calculated adiabatic temperatures as a function of $\mathbb{Z}$ and pressure for TiB_2 (a), ZrB_2 (b), and HfB_2 (c)

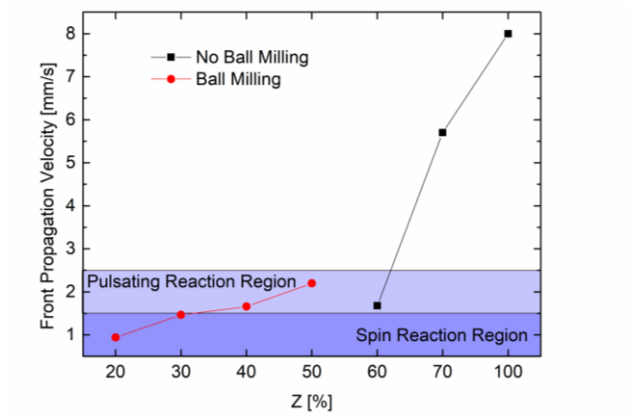

Figure 2: Front propagation velocity measured as a function of Z for the case of TiB_2.

It can be observed that, when no BM treatment was carried out on powder reactants, the front velocity rapidly decreases as $\mathbb{Z}$ is progressively reduced. In particular, a pulsating behavior was manifested by the reaction front when $\mathbb{Z}$ = 60 %. On the other hand, for lower values of $\mathbb{Z}$, the reaction stops to propagate shortly after ignition. The starting mixture was alternatively preliminarily processed by BM, as described in the experimental section. In the latter case, the combined synthesis reaction self-propagated for values of $\mathbb{Z}$ down to 20%, albeit the related front displayed a pulsating or spinning behavior. The corresponding front propagation velocities were in the ranges 1.5-2.5 and 0.5-1.5 mm/s, respectively. The threshold limit of $\mathbb{Z}$ equal to or below which the reaction did not self-propagate was found to be 10%. The extended SHS regime can be likely ascribed to the improved interfaces formation among the starting reactants provided by the BM treatment. The latter one also facilitates the removal of the superficial oxide impurities that typically cover metallic powders. Both these aspects then reduce kinetic limitations apparently present in the synthesis process.

ZrB_2 and HfB_2 systems show a similar qualitative behavior to that displayed by TiB_2. In particular, with no BM, the reaction was capable to self-propagate down to $\mathbb{Z}$ = 70%. In contrast, after the preliminary milling treatment, the SHS character was guaranteed down to $\mathbb{Z}$ = 60%. The synthesis reaction did not self-sustain for $\mathbb{Z}$ values equal or lower than 50 %, regardless of the BM step. In the latter regard, it should be noted that the theoretical predictions foresee values of $\mathbb{Z}_{min}$ of 10-15% lower than those observed experimentally. Such discrepancies could be likely associated to some remaining kinetic limitations, most of which are reduced by the BM treatment. After being pulverized, SHS samples were characterized by XRD, and the obtained results are reported in Figure 3. Specifically, Figure 3a shows that with the process integration of the DR and BR synthesis routes, the desired TiB_2 phase can be produced either after simply mixing initial precursors ($\mathbb{Z}$ = 60 %) or taking advantage of a BM treatment ($\mathbb{Z}$ = 20%-BM). Only slight amounts of oxide impurities (associated to TiO and Ti_2O_3) were detected by XRD, along with the main diboride phase, using the combined DR-BR route, Likewise, Figure 3b and 3c show that the integrated process is able to produce the desired ZrB_2 and HfB_2 phases with minor impurities.
As far as B_2O_3 is concerned, whose presence is expected in the synthesized powders as byproduct according to Eq(2), no boiling likely occurs during SHS under the investigated conditions. The fact that boria was not detected by XRD analyses is explained by its amorphous nature. However, the presence of such an impurity can be evidenced leaving the synthesized powders for 28 days in air, since boria is converted into crystalline boric acid (H_3BO_3). Accordingly, the latter one was detected via XRD on the synthesized powders while, 28 days after a leaching step with distilled water, no trace of H_3BO_3 was found.

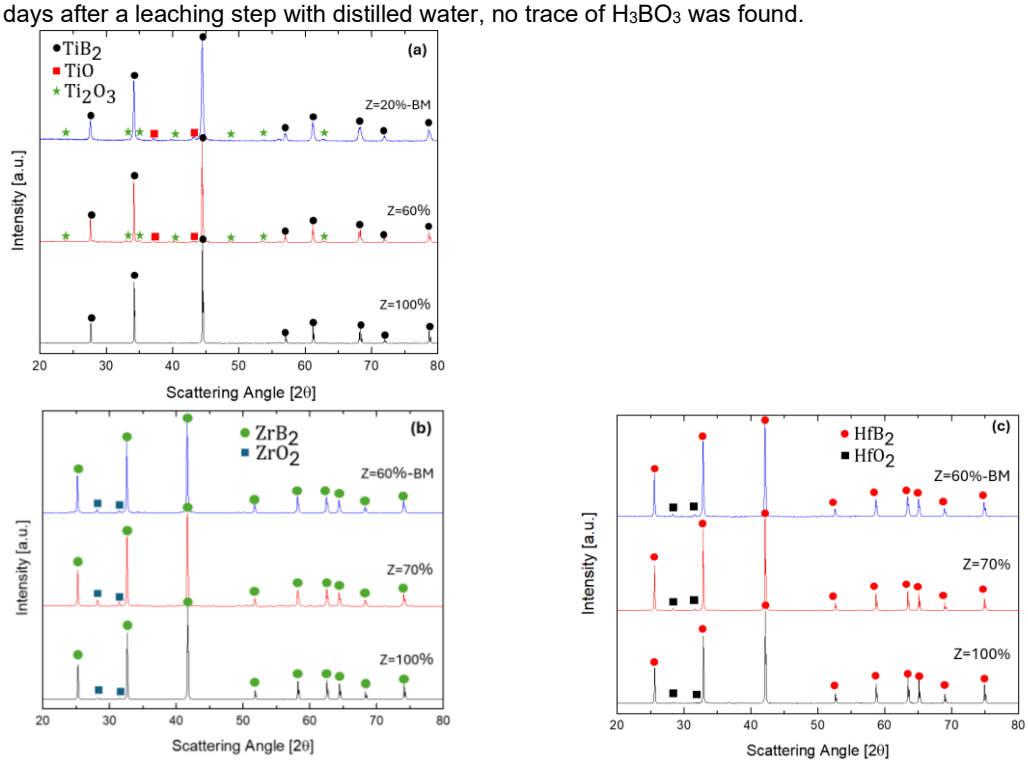

Figure 3: XRD patterns of TiB_2 (a), ZrB_2 (b), HfB_2 (c) systems for the complete direct synthesis, and the last combination for which the reaction self-propagated with and without prior BM.

5. Conclusions

The process integration of the borothermal and direct synthesis reactions for the obtainment of transition metals diborides is proposed in this work. To this aim, a thermodynamic analysis is first performed to predict the optimal conditions for maximising the use of cheaper metal oxides as initial precursors, while guaranteeing a self-sustaining behaviour of the synthesis reaction. With this approach, the heat generated in excess by the strongly exothermic direct reaction can be exploited to sustain the endothermic/low exothermic borothermal one, thus reducing the costs associated to metal reactants and energy consumption. The obtained powders mainly consist of desired diboride phases, alongside with B_2O_3 byproduct, whose presence was removed by leaching it with distilled water. The proposed integrated process is expected to provide considerable economic advantages compared to the individual synthesis routes, which, in turn, could contribute to expand the applications field of such performant Ultra-High Temperature Ceramics.

Nomenclature

A – heat capacity coefficient, J/(mol K)
B – heat capacity coefficient, J/(mol K^2)
C – heat capacity coefficient, J/(mol K^3)
C_P − heat capacity at constant pressure, J/(mol K)
D – heat capacity coefficient, J/(mol K^4)
E – heat capacity coefficient, (J K)/mol
g – molar Gibbs free energy, J/mol
q – molar adsorbed heat, J/mol
P – pressure, bar
T – temperature, K
Z – molar fraction, -

Greek letters:

α – Antoine law parameter, ln(bar)
β – Antoine law parameter, K ln(bar)
γ – Antoine law parameter, K
Δh_f - molar formation enthalpy, J/mol
$\Delta h_{l\to g}$ – liquid to gas molar latent heat, J/mol
Δh_r – molar reaction enthalpy, J/mol
$\Delta h_{s\to l}$ - solid to liquid molar latent heat, J/mol
υ – stoichiometric coefficient, -

Subscripts:

0 – standard reference state
a – adiabatic
b – B_2O_3 boiling
B_2O_3 – referred to boria
g − gas state
i – referred to a generic product
j – referred to a generic phase
l − liquid state
m – melting
MeB_2 – referred to the transition metal diboride
MeO_2 – referred to the transition metal oxide
s – solid state
min – minimum value
max – maximum value

Acknowledgments

M.C. performed his activity in the framework of the PhD in Innovation Sciences and Technologies at the University of Cagliari, Italy. We acknowledge financial support under the National Recovery and Resilience Plan (NRRP), Mission 4, Component 2, Investment 1.1, Call for tender No. 104 published on 2.2.2022 by the Italian Ministry of University and Research (MUR), funded by the European Union—NextGenerationEU—Project Title I-CREATE—Innovative Class of REfrActory ceramics for extreme Environments—CUP F53D23002020006—Grant Assignment Decree No. 104 adopted on 2 February 2022 by the Italian Ministry of Ministry of University and Research (MUR). The financial contribution by Italian Ministry for Research and Education (MUR) under the National Recovery and Resilience Plan (NRRP)—Mission 4, Component 2, “From research to business” INVESTMENT 1.5, “Creation and strengthening of Ecosystems of innovation” and construction of “Territorial R&D Leaders”, project eINS—Ecosystem of Innovation for Next Generation Sardinia (cod. ECS 00000038) is also acknowledged.

References

Barbarossa S., Casu M., Orrù R., Locci A.M., Cao G., Garroni S., Bellucci D., Cannillo V., 2024, Synthesis, Sintering, Mechanical Properties and Oxidation Behavior of (Zr0.5Me0.5)B2 (Me = Ta, Hf) Solid Solutions, Ceramics International, 50, 7, 12158-12166

Barin I., 1995, Thermochemical Data of Pure Substances, 3rd ed., VCH, Germany

Fahrenholtz W.G., Binner J., Zou J., 2016, Synthesis of ultra-refractory transition metal diboride compounds, Journal of Materials Research, 31, 2757–2772

Green D.W., Perry H.R., 2007, Perry’s Chemical Engineers’ Handbook, 8th ed., McGraw-Hill, USA

Guo W.-M., Zhang G.-J., You Y., Wu S.-H., Lin H.-T., 2014, TiB2 Powders Synthesis by Borothermal Reduction in TiO2 Under Vacuum, Journal of the American Ceramic Society, 97, 5, 1359–1362

Kolios G., Frauhammer J., Eigenberger G., 2002, Efficient reactor concepts for coupling of endothermic and exothermic reactions, Chemical Engineering Science, 57, 9, 1505-1510

Licheri R., Musa C., Orrù R., Cao G., Sciti D., Silvestroni L., 2016, Bulk Monolithic Zirconium and Tantalum Diborides by Reactive and Non-reactive Spark Plasma Sintering, Journal of Alloys and Compounds, 663 351-359

Munir Z.A., Anselmi-Tamburini U., 1989, Self-propagating exothermic reactions: The synthesis of high-temperature materials by combustion, Materials Science Reports, 3, 7–8, 277-365

Sani E., Meucci M., Mercatelli L., Balbo A., Musa C., Licheri R., Orrù R., Cao G., 2017, Titanium diboride ceramics for solar thermal absorbers, Solar Energy Materials and Solar Cells, 169, 313 – 319

Wu K.-H., Wang Y., Yu-Yang, Zhang G.-H., Jiao S.-Q., Chou K.-C., 2019, Low temperature synthesis of titanium diboride nanosheets by molten salt–assisted borothermal reduction of TiO2, Journal of Nanoparticle Research, 21, 103